OCUMENTATION PAGE

Form Approved
OMB No. 0704-0188 (2)

k)	2. REPORT DATE	3. REPORT TYPE AND DATES COVERED
	10 NOV. 1992	FINAL 15 Apr 89 - 14 Sep 92

4. TITLE AND SUBTITLE
IN SITU SURFACE STUDIES OF CONVERSION COATINGS FOR STEEL AND ALUMINUM

5. FUNDING NUMBERS
CONTRACT
DAAL-03-89-K-0084

6. AUTHOR(S)
HENRY W. WHITE, FLORIAN MANSFELD AND PAUL BRYANT

7. PERFORMING ORGANIZATION NAME(S) AND ADDRESS(ES)
UNIVERSITY OF MISSOURI-COLUMBIA
COLUMBIA, MO 65211

8. PERFORMING ORGANIZATION REPORT NUMBER

9. SPONSORING / MONITORING AGENCY NAME(S) AND ADDRESS(ES)
U. S. Army Research Office
P. O. Box 12211
Research Triangle Park, NC 27709-2211

10. SPONSORING / MONITORING AGENCY REPORT NUMBER
ARO 26400.7-MS

11. SUPPLEMENTARY NOTES
The view, opinions and/or findings contained in this report are those of the author(s) and should not be construed as an official Department of the Army position, policy, or decision, unless so designated by other documentation.

12a. DISTRIBUTION / AVAILABILITY STATEMENT
Approved for public release; distribution unlimited.

12b. DISTRIBUTION CODE

13. ABSTRACT *(Maximum 200 words)*

The primary goals of the work were to develop mechanisms of corrosion protection for cerium based surface layers on aluminum alloys and on polyacrylic acid (PAA) complexed zinc phosphate conversion coatings on steel. Atomic force microscopy (AFM) using tunnel current control was developed and applied to several problems. The cerium based coatings on Al 6061-T6 are shown to consist of two principle components--a poorly ordered monohydrated aluminum oxide, and an insoluble cerium oxide which forms at areas concentrated with impurities and alloying elements. Electrochemical action during the surface modification process fosters the precipitation of cerium compounds which inhibit further attack. The addition of high molecular weight PAA to the phosphating bath can significantly improve both resistance to corrosion and top-coat adherence of zinc phosphate conversion coatings on steel. Raman spectra showed the compositions of both unmodified and PAA modified films to be zinc phosphate dihydrate. Single crystallite surfaces were imaged using AFM. The morphologies of the unmodified and modified films were in general quite similar, but subtle differences were apparent. Several other projects involving surface layers and adsorbates were carried out and are described.

14. SUBJECT TERMS	15. NUMBER OF PAGES
CONVERSION COATINGS, STEEL, ALUMINUM ALLOYS, ZINC PHOSPHATE, CERIUM BASED TREATMENTS, PROTECTIVE FILMS, INHIBITION, CORROSION, RAMAN SPECTROSCOPY, ATOMIC FORCE	26
	16. PRICE CODE

17. SECURITY CLASSIFICATION OF REPORT	18. SECURITY CLASSIFICATION OF THIS PAGE	19. SECURITY CLASSIFICATION OF ABSTRACT	20. LIMITATION OF ABSTRACT
UNCLASSIFIED	UNCLASSIFIED	UNCLASSIFIED	UL

"IN SITU SURFACE STUDIES OF CONVERSION COATINGS FOR STEEL AND ALUMINUM"

--FINAL TECHNICAL REPORT--

BY
HENRY W. WHITE (UMC), P.I.
FLORIAN MANSFELD (USC), P.I.
AND
PAUL BRYANT (UMKC), ASSOC. P.I.

10 NOVEMBER 1992

U.S. ARMY RESEARCH OFFICE

CONTRACT NO.
DAAL-03-89-K-0084

UNIVERSITY OF MISSOURI (UMC)
COLUMBIA, MO 65211

WITH
SUBCONTRACTS TO
UNIVERSITY OF SOUTHERN CALIFORNIA (USC)
LOS ANGELES
AND
UNIVERSITY OF MISSOURI (UMKC)
KANSAS CITY, MO

TABLE OF CONTENTS

I. STATEMENT OF THE PROBLEM STUDIED

The primary goals of the work were to develop mechanisms of corrosion protection for cerium based surface layers on aluminum and aluminum/silicon carbide metal matrix composites, and on polyacrylic acid (PAA) complexed zinc phosphate conversion coatings on steel. Atomic force microscopy (AFM) using tunnel current control was developed and applied to several problems. Several other projects involving surface layers and adsorbates were carried out, and are described in the section on summary of important results.

Protective coatings on aluminum alloys formed by immersion in dilute aqueous cerium based solutions, and in some cases further treated by polarization in molybdate solutions, have been studied using infrared (IR) and Raman spectroscopies, x-ray analysis, AFM and electrochemical impedance spectroscopy (EIS). These coatings, which are especially resistant against attack by chloride bearing solutions, are shown to consist of two principle components. First, the protective layer largely consists of the poorly ordered monohydrated aluminum oxide, boehmite ($Al_2O_3 \cdot H_2O$, or AlOOH). The other component of the film contains insoluble cerium oxide and forms at areas concentrated with impurities and alloying elements. Electrochemical action during the surface modification process fosters the precipitation of cerium compounds which inhibit further attack.

Raman spectroscopy and AFM were used to investigate the composition and surface structure of zinc phosphate conversion coatings on steel. Zinc phosphate coatings are used extensively to provide corrosion protection and to improve adherence of top coatings to steel. Within the last few years it has been demonstrated that addition of high molecular weight PAA to the phosphating bath can significantly improve both resistance to corrosion and top-coat adherence. The addition of PAA reduces the size of crystallites, which leads to greater film ductility, and therefore to fewer sites for corrosive attack. Organic molecular segments from the PAA are incorporated into the surface structure and provide additional adhesive bonding with polymeric topcoats. Our Raman spectra showed the compositions of both unmodified and PAA modified films to be zinc phosphate dihydrate, $Zn_3(PO_4)_2 \cdot 2H_2O$. AFM was used to measure the morphologies of single crystallite surfaces. Morphologies of the unmodified and modified films obtained by AFM are in general quite similar, but subtle differences were apparent.

II. SUMMARY OF MOST IMPORTANT RESULTS

A. Corrosion Protection by Cerium Based Surface Layers on Al 6061

1. Background: Immersion of Al alloys in rare earth metal chloride solutions for extended periods yields surface layers with protective properties rivaling those of chromate conversion coatings. The original treatment, as developed by Arnott et al.,[1-3] was immersion in 1000 ppm $CeCl_3$ for periods up to a few weeks. They reported that soaking Al 7075-T6 in solutions with small concentrations of cerium salts affected dramatically the surface chemistry and corrosion resistance of the Al alloy. The 4.2 nm thick air grown oxide grew to about 0.5μm after 18 hours immersion in distilled water. Twenty days immersion in 0.1*M* NaCl resulted in many μm of hydrated oxides, but twenty days in 0.1*M* NaCl containing 4m*M* (i.e,.1000 ppm) $CeCl_3$ gave a film only 200 nm thick, which included cerium oxides. Arnott et al. concluded that the protective cerium oxide/hydroxide formation occurred at local cathodic sites, where the locally alkaline conditions

favored precipitation of cerium oxide.[1-3].

Mansfeld et al.[4,5] used electrochemical impedance spectroscopy (EIS) to demonstrate the corrosion resistance of these films on Al alloys and the metal-matrix composites Al 6061/SiC and Al 6061/graphite. The weeks-long soaking treatment was improved by Mansfeld et al.[6] who immersed the samples in hot dilute $CeCl_3$ and $Ce(NO_3)_3$ solutions and added an anodic polarization phase in a sodium molybdate (Na_2MoO_4) solution. The purpose of including $Ce(NO_3)_3$ was to increase the concentration of the cerium ion without increasing the chloride ion concentration which becomes deleterious at higher values. Total treatment time was six hours (6).

2. Samples: The sample substrates were commercially available Al 6061-T6 alloys. Mansfeld et al.[7] demonstrated it was necessary to have an oxide layer for the surface modification to be effective. Samples treated by immersion in $CeCl_3$ after degreasing only, *without* deoxidizing, performed dramatically better than degreased and deoxidized surfaces. The oxide layer is important to the formation or performance of the protective layer. These and later experiences demonstrated that a well formed natural oxide layer was important for the successful formation of the protective layer, and that the quality of the oxide layer on as-received samples was erratic, presumably due to the presence of oils used in the production process and corrosive attack during storage. The variations in oxide quality resulted in highly variable performance of the treated surfaces. A pretreatment process of cleaning, deoxidation and re-oxidation was therefore developed, which resulted in a much more uniform surface prior to the cerium/molybdate treatment. Samples were cleaned in acetone or hexane, water, silicate detergent, and rinsed again in water. They were then deoxidized with either DIVERSAY 560™ (at 30°C for 10 min.) or DEOXIDIZER 17™, (a chromate/HNO_3 bath) then baked at 100°C for 48 hrs. to standardize the surface oxide layer. These pretreated samples, herein referred to as Blanks, were then further treated according to the designations and descriptions in Table I.

Table I. Treatment designations and descriptions for the Al 6061 T6 samples used in this study.

Designation	Treatment
DB1	Blank (deoxidized and baked)
DB2	treated in 5 m*M* $CeCl_3$ at 100°C for 2 hrs
DB3	treated in 10 m*M* $Ce(NO_3)_3$ at 100°C for 2 hrs
DB4	treated in 10 m*M* $Ce(NO_3)_3$ at 100°C for 2 hrs. and in 5 m*M* $CeCl_3$ at 100°C for 2 hrs
DB5	treated in 10 m*M* $Ce(NO_3)_3$ at 100°C for 2 hrs, followed by polarizing in 0.1M Na_2MoO_4 deaerated with N_2 at +500 mV(SCE) for 2 hrs at room temperature
DB6	treated in 10 m*M* $Ce(NO_3)_3$ at 100°C for 2 hrs, in 5 m*M* $CeCl_3$ at 100°C for 2 hrs, followed by polarizing in 0.1M Na_2MoO_4 deaerated with N_2 at +500 mV(SCE) for 2 hrs at room temperature
DB7	treated in distilled water at 100°C for 2 hrs

3. Results and Discussion: *IR*--Figure 1 shows FT-IR spectra taken for a series of samples. With the exception of the untreated sample, Fig. 1(a), there is a remarkable similarity among the varieties of treatment. The most notable feature is due to water, here exhibiting the characteristic strong, broad O-H stretch mode with peaks near 3100 and 3300 cm^{-1}, which is lower than for liquid water, and the weaker structure at about 1600 cm^{-1}, due to the H-O-H bending mode of molecular water. The sharper feature at 1080 cm^{-1} is usually attributed to an Al-OH librational mode, characteristic of boehmite ($AlOOH = Al_2O_3 \cdot H_2O$) which typically forms on aluminum in hot water.[8] For well crystallized boehmite this band appears as a doublet at 1080 and 1150 cm^{-1}, with the former much more intense. Poorly ordered boehmite, or pseudoboehmite, exhibits only a band at 1080-1090 cm^{-1}. The overwhelming spectral signature is thus attributed to poorly ordered boehmite for all samples.

Some of the structure around 1600 cm^{-1} in the spectra is due to molecular water in the film. This water also contributes to the O-H band above 3000 cm^{-1}, although the greatest contribution in this higher energy region is due to hydroxyls in a boehmite-like structure, rather than for O-H groups in molecular water. Other structure in these spectra is likely due to various non-boehmite oxides of Al and to vibrational modes of the hydroxyl group other than the stretching mode.

The IR spectra for the treated films showed no evidence for any of the anions known to be present in the processing solutions--cerium, nitrate, chloride or molybdate.

Raman--Soaking 1 μm anhydrous α alumina particles in 3 m*M* $CeCl_3$ resulted in no changes in the Raman spectrum of the alumina. It was hypothesized that if the Ce had an affinity for normal sites occupied by the Al, then a high surface area sample such as 1 μm alumina would spectroscopically demonstrate this substitution. The motivation for using this particular form of alumina was to approximate the amorphous, anhydrous oxide layer that occurs on a naturally oxidized sample. The small particles present a variety of crystal faces to the solution with many potential adsorption/substitution sites, which would allow incorporation of Ce ions into the alumina structure if this process were allowed.

In general, Raman spectroscopy was problematic for this study. In most cases spectra of the films showed either nothing or only very weak features on top of a broad, but not strong, flourescence background. One set of samples did yield significant spectra much like those obtained by FT-IR. After aging in air for a few days they became consistent with the large majority of samples in this study and showed no useful Raman spectra. Other sets of samples did not show this change in behavior. We attempted to understand the reasons for this change for this one set of samples, but were unsuccessful.

Some of the Raman spectra are shown in Fig. 2. The strongest feature is near 1050 cm^{-1} and may be associated with the peak near that energy in the FT-IR spectrum of boehmite. In Raman spectroscopy the nitrate ion, $(NO_3)^-$, has a strong peak (ν_1) near 1020 cm^{-1}, and $(MoO_4)^{2-}$ has its dominant peak (also ν_1) near 890 cm^{-1}. These peaks should not be infrared active and cannot be invoked in the FT-IR data. Curves (b), (c) and (d) in Fig. 2 all show peaks near 1060 cm^{-1}. These peaks cannot be associated with a nitrate ion since the treatment for the sample for Fig. 2(b) did not contain cerium nitrate.

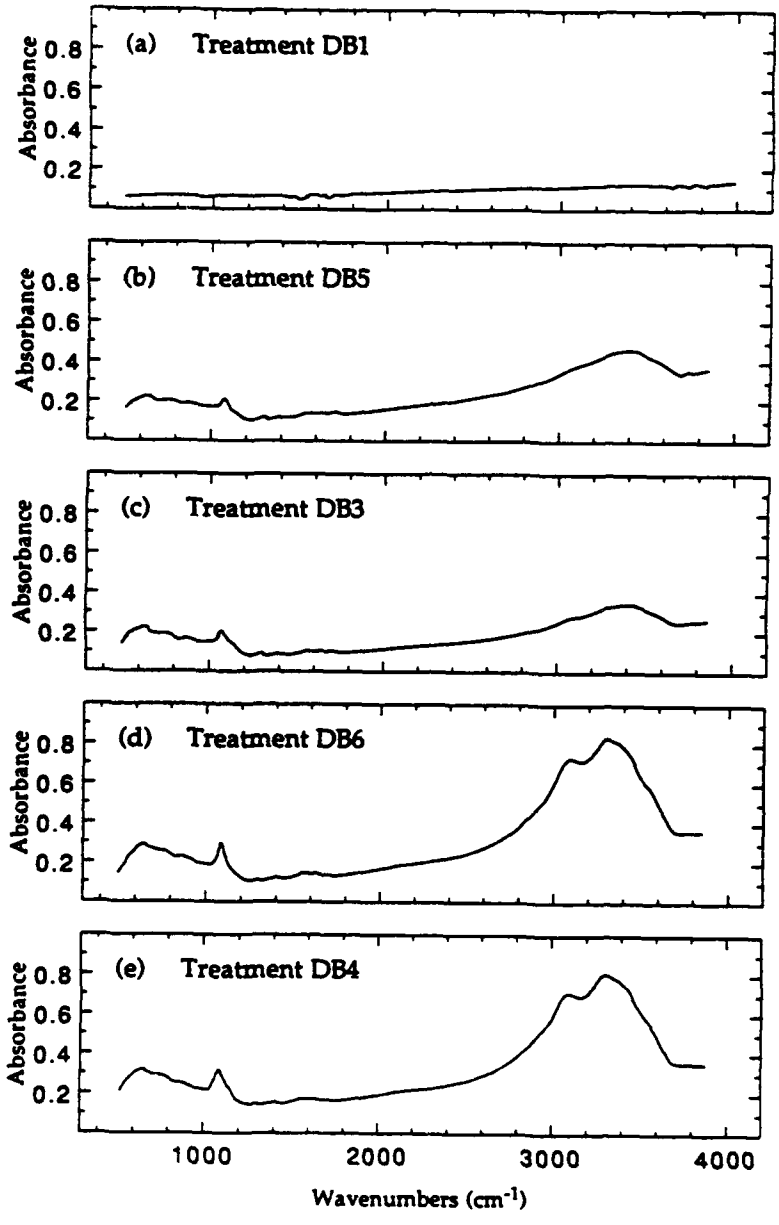

Fig. 1. FT-IR spectra for Al 6061-T6 surfaces with treatments as designated and described in Table I. The structures in spectrum in (a) near 1600 and 3700 cm^{-1} are spurious, due to low signal strength. The spectra in (b) through (e) are consistent with a poorly ordered boehmite structure.

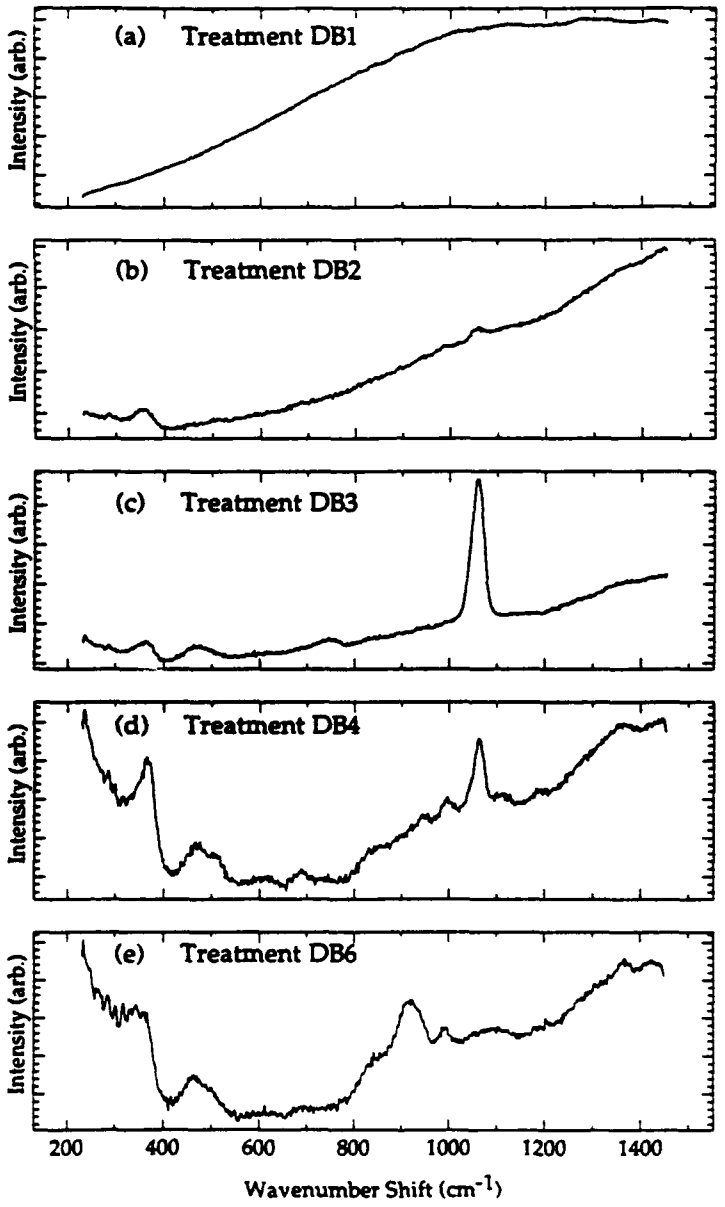

Fig. 2 Raman spectra for Al 6061-T6 surfaces with treatments as designated and described in Table I.

The major peak near 910 cm^{-1} in Fig. 2(e) may be due to the molybdate ion, although shifted to slightly higher energy than when occuring in either the aqueous or solid form. It is impossible to be certain for this assignment with the limited information available.

X-ray—Examination of the treated surfaces with either an optical or an electron microscope showed localized deposits on the surface. These features were approximately circular with diameters up to 10 μm, but averaging about 3 μm. A typical 50 μm x 50 μm area had approximately 20 such features. They were present on all samples except for the Blanks.

Elemental x-ray signals from the unblemished regions of the treated samples were overwhelmingly those for Al, as shown in Fig. 3(a) and 3(c). Spectrum (a) in Fig. 3 is for a Blank without cerium or polarization treatments, but with boiling in distilled water for two hours. No features other than those for the Al photoelectron are seen. As such, its features in the 4 to 8 KeV region are representative of the signal recorded over *unblemished* regions of the surface for samples treated in cerium solutions. To illustrate, the spectrum in (c) is from a sample treated with cerium nitrate and cerium chloride in a region of the surface without a cerium-rich deposit. The cerium-free region, as determined by these x-ray data, includes at least 90% of the surface of any sample.

Elemental x-ray signals obtained when the probing electron beam was focused on a cerium-rich deposit revealed an abundant variety of other elements, including Ce, Si, S, Mo and Cu. Representative curves are shown in Fig. 3(b) and 3(d). The only consistently present element, however, was Ce, although Fe was regularly dominant, as illustrated in spectrum (d).

The x-ray data consistently showed Ce to be located in regions where there was sufficient chemical variety that interesting phenomena would occur if water were to be present. These sites generate the conditions favorable to the precipitation of insoluble cerium compounds. Arnott et al.[1] used Auger electron spectroscopy to probe the elemental composition of the films. Unfortunately, the probe spot size was approximately 100 μm diameter, much larger than the average size of the interesting cerium-rich surface features identified in this study. As a consequence, Arnott et al.[1] averaged the cerium-rich sites with areas containing much lower concentrations of cerium, thereby not detecting the cerium-rich sites.

AFM—AFM images of a series of untreated and treated Al 6061 samples were recorded with a Nanoscope II for areas ranging from 15 x 15 μm^2 down to 100 x 100 nm^2. The morphologies of the films, when viewed at scales representative of the film structure, are independent of the treatment process, consistent with the spectroscopic evidence. Figure 4 shows representative AFM views of these films. Image (a) is a 500 nm x 500 nm area for treatment DB1, a Blank. Image (b) is the same size scan for a sample with treatment DB4, which includes $CeCl_3$ soaking. Image (c) is also the same size scan for a sample with treatment DB6, which includes soaking in cerium nitrate and cerium chloride solutions followed by anodic polarization in a molybdate solution. Image (d) is a 10,000 nm x 10,000 nm scan for the sample with treatment DB6. Considering the variety of treatments, it is surprising that the surface structures of these films are so similar. All AFM images show the surface to be composed of an aggregation of "pillow-like" formations ranging from about 50 nm to 200 nm in size.

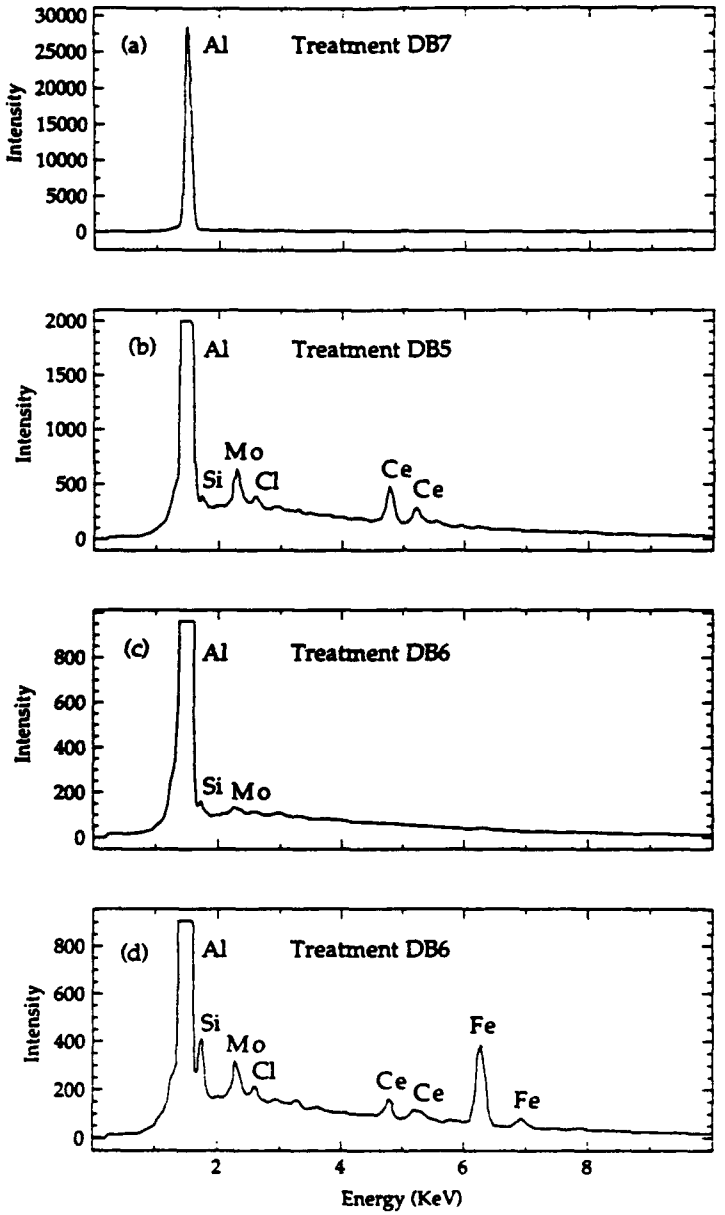

Fig. 3. Energy dispersive x-ray analysis for Al 6061-T6 surfaces with treatments as designated and described in Table I. Spectra (a) is for a sample without cerium or polarization treatments. Curves (b) and (d) are representative of the signals recorded when the probing electron beam is focused on a cerium-rich deposit. The spectrum in (c) is from a sample treated with cerium nitrate and cerium chloride in a region of surface without a cerium-rich deposit.

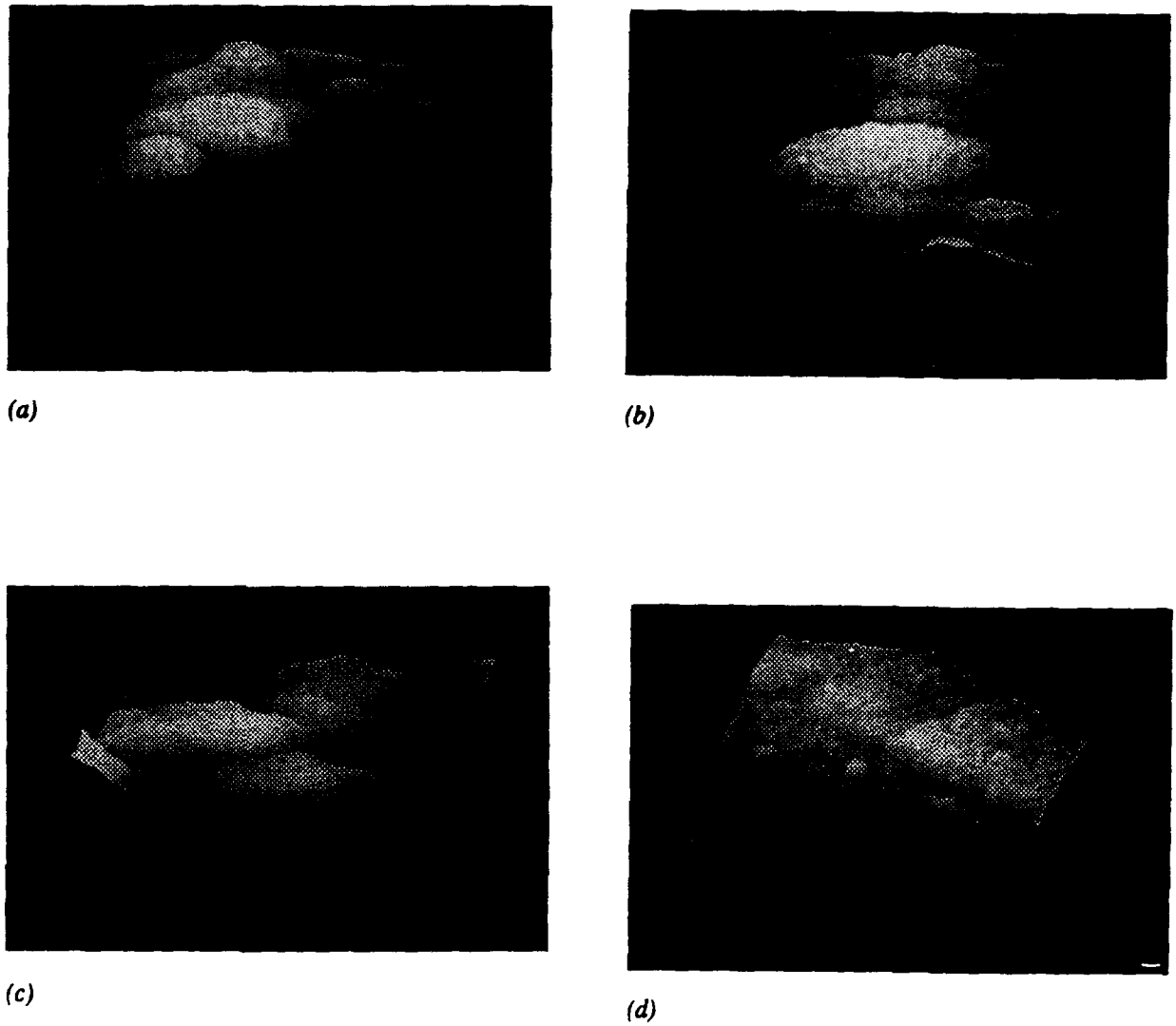

Fig. 4. AFM images for Al 6061-T6 surfaces with treatments as designated and described in Table I. Image (a) is a 500 nm x 500 nm area for treatment DB1, a Blank. Image (b) is the same size scan for a sample with treatment DB4, which includes $CeCl_3$ soaking. Image (c) is also the same size scan for a sample with treatment DB6, which includes soaking in cerium nitrate and cerium chloride solutions followed by anodic polarization in a molybdate solution. Image (d) is a 10,000 nm x 10,000 nm scan for the sample with treatment DB6.

EIS— EIS showed that treatment DB6, i.e., with $CeNO_3/CeCl3/Na_2MoO_4$, was the most effective treatment. Uniform corrosion was very low and localized corrosion did not occur after treatment DB6 during exposure to 0.5*N* NaCl (open to air) for 60 days. The use of cerium nitrate in combination with cerium chloride allows an increase in cerium cation absorption without a further increase in the Cl concentration. Clearly, some Cl ion is needed to optimize the process, but too much Cl ion is counterproductive, since it causes too much localized corrosion during the surface treatment. Preliminary studies have indicated that there is a synergistic effect of Ce and Mo, i.e., treatment in Ce solutions or polarization in the Mo solution alone did not produce the excellent corrosion resistance obtained in the combined Ce-Mo treatment.[9]

4. Conclusions: Reflectance IR studies of the same samples used in the AFM studies indicate that the water and hydroxyl content in the surface layers was increased during the treatment process. These and other features in the spectra relating to the structure of the hydrated aluminum oxide are uniform for the variety of treatments of the surface, indicating that there is no large scale chemistry being driven by the various treatments, but that treatments in the cerium and molybdate solutions create changes in the physical and chemical structure of the protective surface in relatively subtle fashion. It is important to note that these changes occur predominantly at chemically active sites on the surface.

Our model of the surface is that of poorly ordered boehmite, the expected product of aluminum treated in hot water, interspersed with deposits of insoluble cerium(III) oxides[10] whose presence is dictated by the chemical activity at impurity sites, or at sites with enhanced concentrations of alloying elements. This presence of cerium serves as a barrier to further attack at these particularly active sites, which would otherwise serve as initiation sites of pits and continuing sources of aluminum ions for the production of various aluminum oxides and hydroxides. Smaller concentrations of cerium present in the boehmite phase of the film may inhibit thickening of this component by combining with tetrahedrally coordinated Al ions at active sites, thereby restricting further growth.

Results from the different techniques employed in this study are uniform in support of this model which is consistent with previous studies, although the present study provides much more specific information about the two-component nature of the film. None of the data can be interpreted to suggest that these results and the mechanisms of protection should not apply to other Al alloys. Treatment with cerium and molybdate solutions as described here should passivate active sites at which pits could initiate by the formation of cerium oxides for all Al alloys. The actual composition of the treatment solutions might have to be adjusted for optimum results depending on alloy chemistry. Preliminary results for Al 7075-T6 suggests that the $CeCl_3$ step has to be eliminated because it causes pitting for this high Cu content alloy.[9]

B. Raman Spectroscopy and Atomic Force Microscopy Studies of Zinc Phosphate and Polyacrylic Acid Complexed Zinc Phosphate Conversion Coatings on Steel

1. Background: Crystalline zinc phosphate films have been used extensively for many years to protect cold-rolled steel against corrosion and to provide a good substrate for paint adhesion. The films are grown in a phosphoric acid bath containing zinc phosphate at elevated temperatures.

Crystallites 10 to 20 microns in size form within a few minutes, yielding a film several microns in thickness. Corrosion protection is good, especially if the surface is completely covered. Recipes can be tailored to obtain reproducible films with complete coverage on various steels, but a given recipe may not always give good protection for all steels. High quality films with good coverage are more easily attained for low carbon steels than for those with high carbon content. Difficulties obtaining uniform coverages have been noted for some low-grade reclaimed (mixed) steels.

Several efforts to characterize zinc phosphate films have been reported. Ghali and Potvin[11] explored the mechanisms associated with different steps during film growth. They measured the relative abundance of iron and zinc in the films and noted that the iron content dropped dramatically with time of growth. They and earlier workers concluded the outer film to be trizinc orthophosphate tetrahydrate, hopeite $Zn_3(PO_4)_2 \cdot 4H_2O$. More recently, Sugama et al.[12,13] used a number of surface analytical techniques to further investigate mechanisms of film growth and structure. A three layer structure was proposed, with the outermost layer being zinc phosphate dihydrate, $Zn_3(PO_4)_2 \cdot 2H_2O$.

In an effort to improve the corrosion protection capabilities of zinc phosphate coatings, Sugama et al.[12,13] grew films with selected high-molecular-weight organic acids added to the phosphating bath. Ordinary phosphate films are subject to cracking, which provides sites for corrosive attack. They conjectured that segmented organic acid groups in the bath might provide additional nucleation sites for crystallite growth, thereby leading to a film with smaller crystallites and greater strength during flexure. The decreasing crystal size, they believe, is due primarily to segmental chemisorption to the precipitated crystal surfaces of functional electrolyte groups such as carboxylic acid (-COOH) and sulfonic acid ($-SO_3H$).

Sugama et al.[12,13] found poly(acrylic acid), herein referred to as PAA, with a molecular weight in the neighborhood of 50,000 significantly improved corrosion protection. The PAA molecule has a polyelectrolyte character. Its structure is, $[-CH_2CH(COOH)-]_n$, and can be considered as consisting of a hydrophobic main chain $(-CH_2-CH-)_n$ and hydrophilic carboxylic acid pendent groups (COOH).

The goals of this work were to characterize and compare surface properties of unmodified zinc phosphate films and zinc phosphate films modified with PAA using Raman spectroscopy and atomic force microscopy (AFM). In particular, evidence for the presence of PAA or organic functional species from the PAA in the modified films was sought.

2. Samples: Films were grown following recipes as reported by Sugama et al.[2,3] For example, a 1.0 wt. % PAA film would be prepared as follows: The steel sample is wiped with acetone-soaked tissues to remove any surface contamination due to mill oil. The steel is then immersed for up to 15 min. in the conversion solution consisting of 5 g zinc phosphate ($Zn_3(PO_4)_2 \cdot 2H_2O$), 10 g (85% H_3PO_4 solution), 360 g water and 16 g (25% PAA) at a temperature of 90°C. After immersion, the surface is rinsed with water, and then dried in an oven at 150°C for 15 min. to remove any moisture from the deposited conversion film surface and to solidify the PAA macromolecules. Numerous unmodified and modified films were grown under a variety of conditions, with PAA contents ranging from 1 to 5 wt. % in the modified films. Some films were baked at various elevated temperatures up to 150°C, and others left unbaked to determine the effect of baking on

surface properties.

A Nanoscope II system with contact type AFM heads, and a Nanoscope III system with both contact and non-contact type AFM heads, both from Digital Instruments, Inc.,[14] were used to obtain images on unmodified and modified films. The tips are located on the end of a thin triangular shaped cantilever which has a Au reflective coating. SiN tips were used in this work.

For both "contact" and "non-contact" AFM the position of the tip is sensed optically; however, in for non-contact AFM the tip is also vibrated and held just above the surface. The sample surface is detected by oscillating the cantilever at or near its natural frequency and then approaching the surface with the tip. The Van der Waals force gradient due to the tip-surface interaction modifies the spring constant of the cantilever and shifts its resonant frequency. The amount of shift is used to track the sample surface during scan. Non-contact AFM is particularly useful for obtaining images of soft and deformable surfaces. Nanoscope III images were taken by S. Manalis at Digital Instruments, Inc.[14]

Imaging with STM was attempted but the tunneling current generated was not sufficient to obtain images.

3. Results and Discussion: The Raman spectra are shown in Fig. 5. Spectrum (a) is from $Zn_3(PO_4)_2 \cdot 2H_2O$, zinc phosphate dihydrate, as received. Spectrum (b) is from a zinc phosphate film grown with no PAA in the solution bath. spectrum (c) is from a modified film with 2% PAA. The Raman spectra of the surface and the micro-Raman spectra of individual crystallites demonstrate clearly that the surface film is composed, overwhelmingly, of crystallites of zinc phosphate dihydrate, $Zn_3(PO_4)_2 \cdot 2H_2O$.

With micro-Raman we were able find evidence for two other species on the surface of films modified with PAA. One species was conjectured to be some form of hydrated iron oxide or iron phosphate. The source of these spectra was an inclusion, somewhat transparent, but brown tainted. The other species detected by micro-Raman spectra were obtained from inclusions on the surface of modified films were clear and more island-like.

IR spectra from the surface of PAA modified films showed no evidence for organic groups.

AFM images showed a number of interesting structures and features. All AFM images were taken on relatively flat "plateaus" associated with individual crystallites. These crystal faces were parallel to the steel substrate surface. While differences between the unmodified and the PAA modified films could be observed, the general morphologies of the two types of films are similar. The significant features imaged were long striations, with a cross-striation pattern. Some differences were observed which may be associated with addition of PAA to the phosphating bath.

AFM images were taken with a Nanoscope II system and a Nanoscope III system. One difference between the images taken with the two systems was that those taken with the Nanoscope III system revealed rectangular shaped pits on both modified and unmodified films. Individual differences in tip shape may be an important parameter in explaining the fact that pits were detected in images taken with the Nanoscope III, but not detected for images taken with the Nanoscope II system.

AFM images obtained with the NanoScope II in contact mode on unmodified films are shown in surface view in the four half-tones labeled Fig. 6(a) - 6(d). Similarly, AFM images obtained with a Nanoscope II on a film modified with 5% PAA are shown in surface view in Fig. 7(a) -

7(d). AFM images obtained with the Nanoscope III on unmodified and modified films are shown in top view in Fig. 8(a) - 8(d).

A large number of pyramidal shaped pits in addition to the striation patterns were observed in AFM images taken with the Nanoscope III, for both contact and non-contact modes. For the areas scanned, the pyramidal shaped depressions were much more prevalent on the PAA modified sample as on the unmodified sample. The Nanoscope II images showed far fewer depressions, and they were without a regularized shape. The orientation of pyramidal edges was not fixed along the direction of scanning, indicating the pits were not tip artifacts. On any given scan, however, the orientations of pit edges were in registry with one another, which would not be unexpected for defects associated with a common aspect of crystalline growth.

The surfaces did appear rough. The standard deviations for both unmodified and PAA modified surfaces were typically in the range of 10 to 20% of the surface height range.

Atomic resolution AFM images could not be obtained. The AFM images shown in Figs. 6 and 7 were taken with a scan head with a 15 μm x 15 μm maximum scan size. A second AFM head with a smaller range, 0.8 μm x 0.8 μm, was also used. This smaller scan head is capable of higher resolution, primarily due to its greater mechanical stability, but images recorded using the smaller head were no clearer. On suitable samples either of these heads are capable of resolution approaching atomic scale. Thus, the inability to record higher resolution images suggests the resolution obtained was limited by subtleties associated with interactions of the tip with the sample surface. Possibilities include elastic deformation of the surface by the probing tip, electrostatic charging due to the contact of the tip with the surface, surface debris such as molecular segments from the PAA, or capillary condensation of water in the constriction formed by the tip and sample surface.

Non-contact AFM gave higher resolution than contact AFM. When using the Nanoscope III system on a PAA modified film, the non-contact AFM was able to image 10-20 nm surface features. Features this small could not be imaged with contact AFM. A possible explanation for the difference in resolution is that the modified surface may have soft or sticky features, and these features were being distorted by the tip when using contact AFM.

4. Conclusions: The preponderance of crystallites on the surface of both the unmodified and PAA modified surfaces were zinc phosphate dihydrate as evident from the Raman and micro-Raman spectra.

The surfaces of the individual crystallites investigated were rough and non-periodic. AFM was successful in obtaining surface morphologies of single crystallite surfaces for both unmodified and modified films. The AFM images for the two surfaces show qualitative differences in morphology, although both are characterized by long striations with widths from less than 100 nm up to several 100 nm. Rectangular shaped pits were quite apparent in AFM images taken with the Nanoscope III system. For the surface areas investigated, the surface density of pits was higher for the modified films than for unmodified films. The common orientation of pit edges within a scan on a crystallite suggests the mechanism of pit formation is intimately related to the mechanisms of crystal growth and structure.

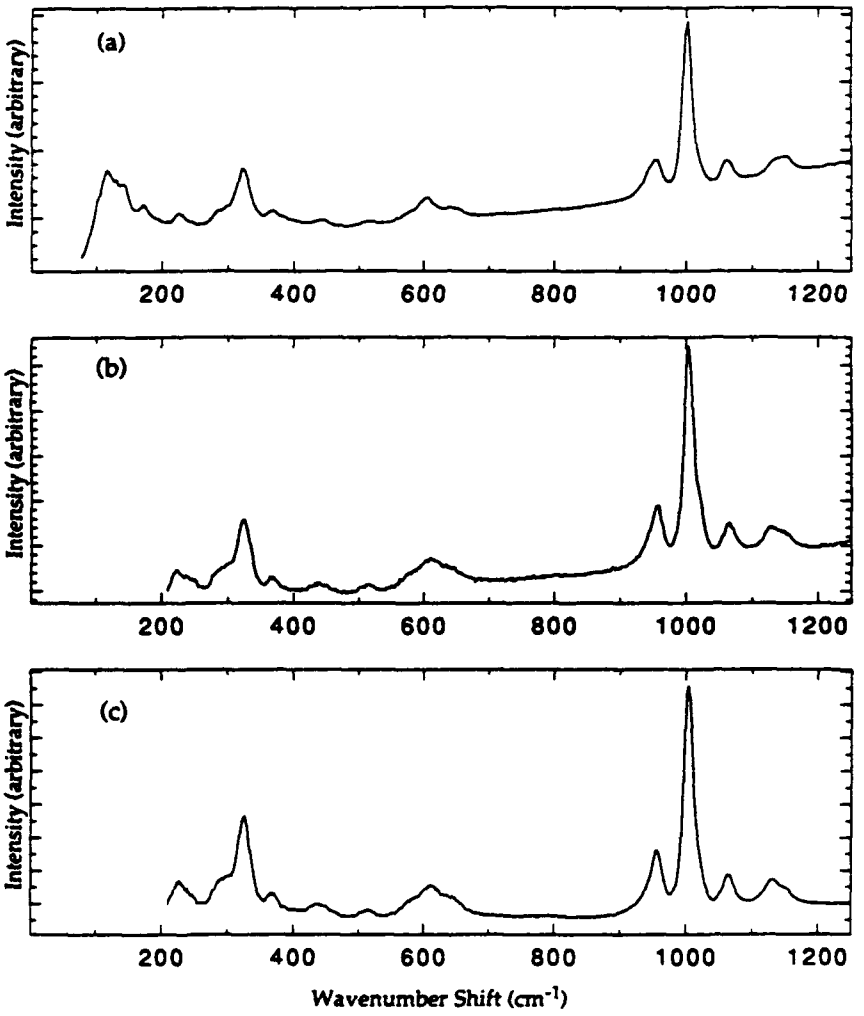

Fig. 5. Representative Raman spectra used to identify surface crystallites. Spectrum (a) is from $Zn_3(PO_4)_2 \cdot 2H_2O$, zinc phosphate dihydrate. Spectrum (b) is from a zinc phosphate film grown without PAA. Spectrum (c) is from a modified film with 2% PAA in the bath.

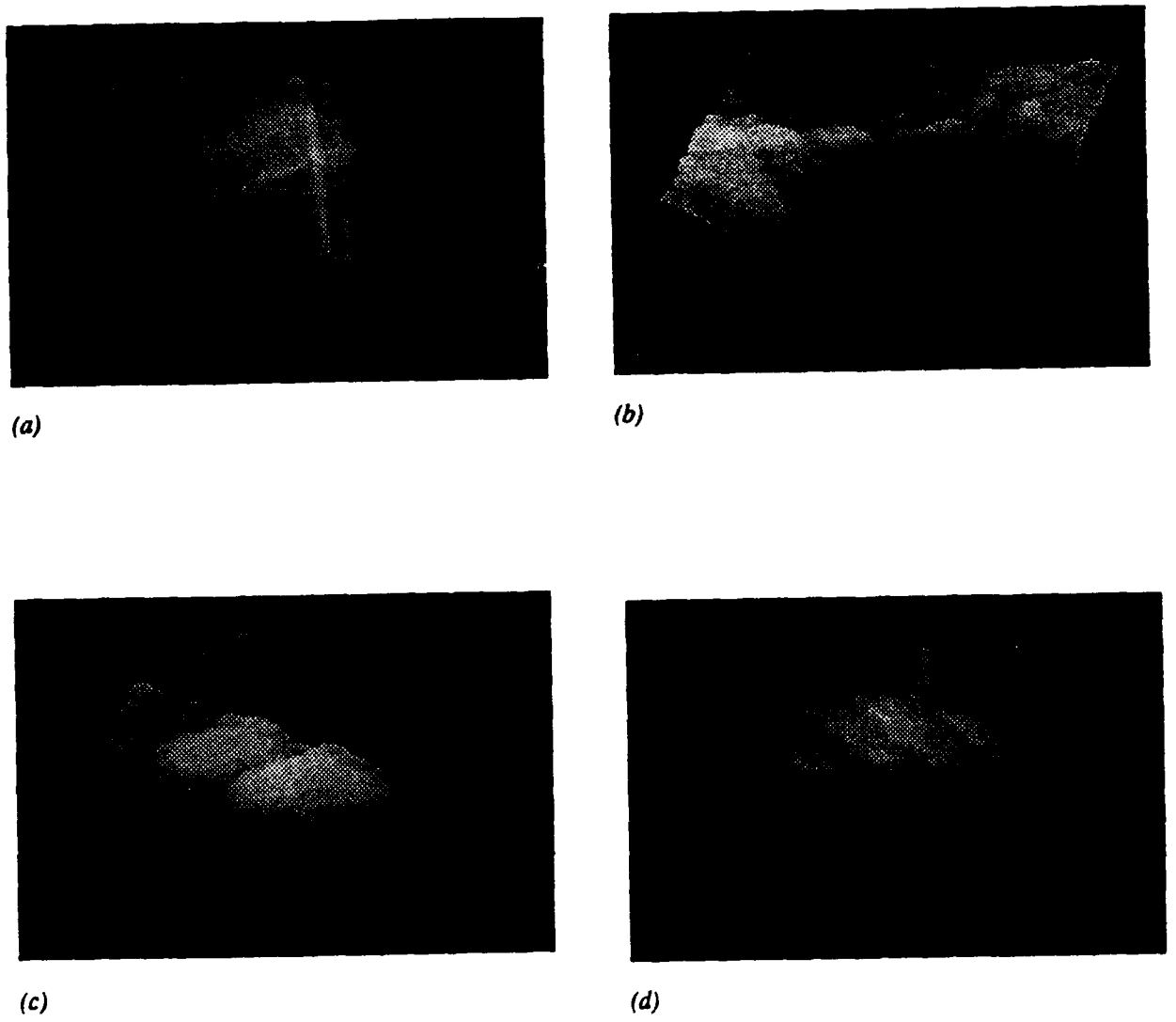

Fig. 6. Contact AFM images obtained on an unmodified zinc phosphate film taken with a Nanoscope II. Surface views are shown. Image (a) is a 2 μm x 2 μm sub-image, taken from a 5 μm x 5 μm scan. Major striations as well as smaller striation-like features perpendicular to the major ones are prevalent. Note the sharp protrusions. Image (b) is a 500 nm x 500 nm scan taken in the neighborhood of the scan for image (a). It reveals in greater detail the small structure perpendicular to the main striations. Image (c), 350 nm x 350 nm, shows a close-up of a "cross" in images (a) and (b). Image (d) is a 1 μm x 1 μm scan from a region which is extremely flat. A close-up of one of the sharp protrusion can be seen in the upper central portion of the scan.

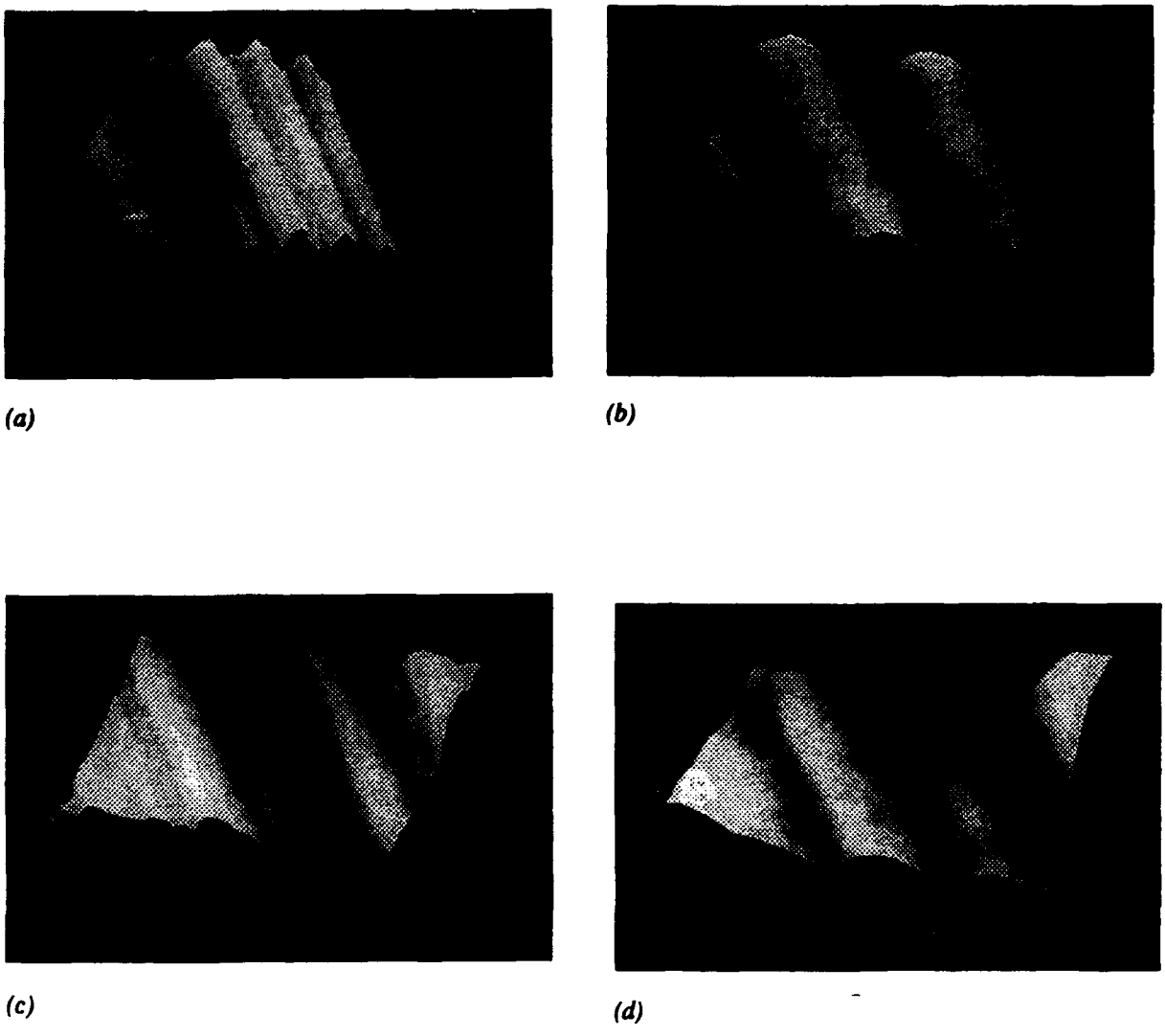

Fig. 7 Contact AFM images obtained on a 5% PAA modified zinc phosphate film taken with a Nanoscope II. Surface views are shown. Image (a) is a 1.5 μm x 1.5 μm scan illustrating the striated pattern prevalent on this sample. Image (b) is a 500 nm x 500 nm scan with more narrow striations than in image (a). Image (c) is a 500 nm x 500 nm scan in a different region. Image (d) is a smaller scan, 200 nm x 200 nm, in the same region as image (c).

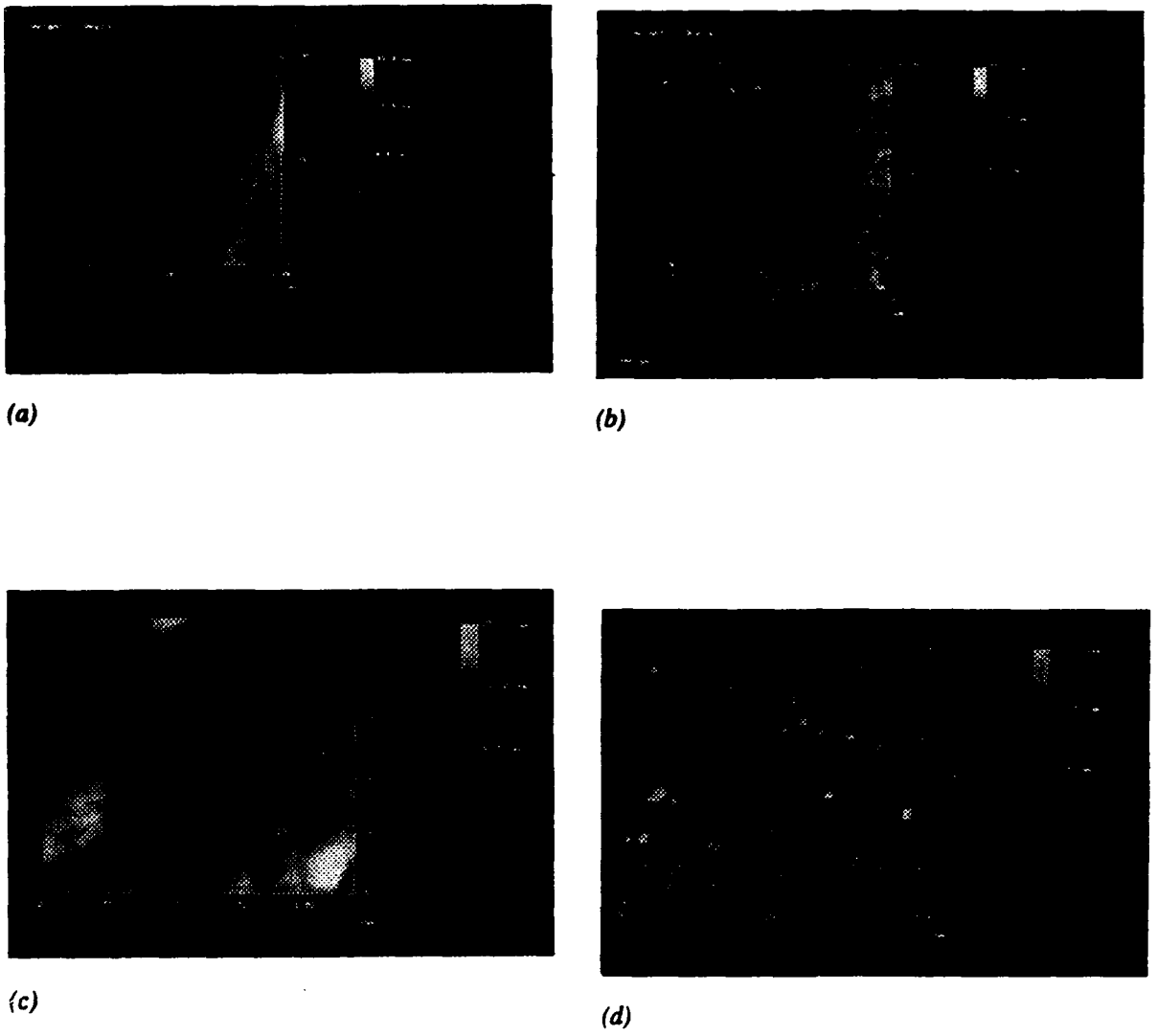

Fig. 8 Contact and non-contact AFM images on zinc phosphate films taken with a Nanoscope III. Top views are shown. Image (a) is a 2 μm x 2 μm scan of an unmodified film using contact AFM. Image (b) is a 2 μm x 2 μm scan of a modified film using contact AFM. The surface number density of pits is greater for the modified film than for the unmodified film, as shown in (a). Image (c) is a 125 nm x 125 nm scan of a modified film using non-contact AFM. The resolution is higher than could be obtained using Nanoscope III contact AFM. Image (d) is a 500 nm x 500 nm scan of an modified film using non-contact AFM. The surface features appear similar to those in image (b), but at higher resolution.

Specific organic molecular segments could not be identified in the AFM images, even though the apparent resolution appeared sufficient to allow large entanglements to be imaged. Higher resolution could be obtained with non-contact AFM than with contact AFM when investigating modified films using the Nanoscope III system. These differences can reasonably be ascribed to the different growth conditions in the phosphating baths, i.e., with and without PAA. The presence of the PAA would increase the number of nucleation sites and thereby increase the number of defect sites, such as pits. IR results were not helpful in identifying PAA on the surface.

In summary, the spectroscopic and microscopic evidence for the presence of molecular segments from the PAA on or in the crystallites for the modified films is weak at best. One possibility is that PAA segments preferentially adsorb on crystal faces other than the dominant plane, which is in the plane of the sample surface. It is quite possible that the PAA has a stronger affinity for the side facets of the crystallites. Thin (i.e., a molecule or two thick) but more or less complete coverage by PAA there would have be consistent with the a very weak Raman and IR signature, but could easily influence the growth of the crystallites and have the pronounced adhesion improvements for top-coatings.

C. Cerium Treated Al/SiC Metal Matrix Composites

Raman and micro-Raman spectra taken at UMC of pristine and surface modified Al/SiC metal matrix composites (MMC) prepared at USC showed a significant contribution due to crystalline silicon, as distinguished from SiC, in most treated samples compared to pristine samples. The apparent presence of significant amounts of Si may impact the performance of the composite. Strong evidence exists for the presence of other species, also, which may evolve during the hot press fabrication of the MMC. AFM images are currently being obtained at UMC to complement the Raman data, and a manuscript is being prepared for publication.

Note on Al./C: Al/C interfaces were prepared at UMC using vacuum evaporation, and were analyzed before and after exposure to corrosive or cerium-based solutions for corrosion protection. Thin Al films on carbon substrates were completely removed upon exposure to water (pH 2-11), but when soaked in a solution of dilute aqueous $CeCl_3$ (pH 7) the films became highly resistant to dissolution, as evidenced by surface Raman spectra. The MMC industry has evidently abandoned efforts to produce Al/C MMC on a commercial basis, in part due to perceived unsurmountable difficulties in process control during manufacture and to corrosion prevention and control in the field. Commercial samples are not available. Accordingly, our efforts were directed to other projects in the proposed work.

D. Modification of Al Alloys in Molten Salt Mixtures for Corrosion Protection

A new effort in surface modification of Al alloys has been initiated at USC in which the treatment is carried out in molten salt mixtures between 200 and 300°C. The experimental apparatus for performing electrochemical in-situ measurements in molten salts has been assembled. In the initial phases of this task Al 6061 has been immersed in a $SnCl_2$-NaCl salt mixture with or without $CeCl_3$ for two hours. Polarization resistance and impedance measurements have been performed. Polarization curves have also been recorded during immersion in the molten salt.

From these curves kinetic parameters such as Tafel slopes and the corrosion rates can be obtained as a function of immersion time. The corrosion resistance of the treated samples has been tested during immersion in 0.5 N NaCl. Samples have been prepared for surface analysis by EDAX and AES. The analysis of the electrochemical data is being carried out at present. Preliminary results indicate that immersion in molten $NaCl/SnCl_2$ increases the corrosion resistance of Al 6061 probably by increasing the thickness of the oxide film. Additional resistance to localized corrosion results from the incorporation of cerium oxides in the oxide film.

E. Development of AFM with Tunnel Current Control

A new AFM design which utilizes the high sensitivity of a tunnel junction has been developed by P. Bryant and co-workers at UMKC. It has been successfully applied to physical and biological samples, including protein chains. This work has been accepted for publication in J. Vac. Sci. Tech. (**A8**, 3502 (1990), and **A10**, 641 (1992)), and another manuscript has been submitted to JVST. These manuscripts describe construction and calibration of AFM levers, applications such as simultaneous operations of STM and AFM, and high resolution imaging. Attempts were made to image $Zn_3(PO_4)_2 \cdot 2H_2O$, but without success.

F. STM of Solid C_{60}/C_{70}

We have measured and reported (*Nature* **348**, 623-24, 13 Dec. 1990) direct imaging of C_{60} molecules in sub-micrometer sized particles of fullerite using STM. The images reveal spherical molecules, spaced about 1 nm apart, stacked in close-packed arrays. Our results give a direct demonstration of the highly symmetric structure of these clusters. Such molecules and clusters are thought to play an important role in soot formation, and may have applications in catalysis, lubrication, fabrication of high performance coatings with ultra-low hydrogen contamination, or selective transport of caged atoms.

G. Raman Studies of the Conducting Polymer Polyaniline

Measurements carried out in collaboration with co-workers at UMC (Bradford, Cowan and Marrero) used *ex situ* and *in situ* Raman spectroscopy to investigate the influence of moisture on the electrical conductivity on polyaniline. It demonstrated the capability of the newly constructed Raman spectrometer to obtain spectra on films of 5 nm thickness under *in situ* electrochemical conditions. A preliminary report of this work is in Bull. Am. Phys. Soc. 35, 197 (1990).

H. Micro-Raman Attachment Upgrade

The Raman system at UMC was upgraded by addition of a micro-Raman attachment in October 1990. The design, provided by J. Butler, NRL, is based on a commercially available optical microscope, modified to accept and focus the incident laser beam and to collect the beam with the same objective optical system. Spot size of the incident beam is on the order of one micron diameter. High quality spectra have been obtained on individual surface crystallites a few microns across, as discussed above. Funds in the amount of $15,427 to purchase these items were provided by the University of Missouri Weldon Spring Fund.

I. Scanning Probe Microscopy Upgrade

The Nanoscope II STM system at UMC was upgraded by addition of an AFM and electrochemical STM and AFM units in March 1992. The AFM unit was used extensively to obtain images of cerium based surface layers on aluminum alloys and on unmodified and PAA modified zinc phosphate coatings on steel. Funds in the amount of $47,900 to purchase these items were provided by the University of Missouri.

III. PUBLICATIONS AND TECHNICAL REPORTS

"Characterization of Diamond and Diamond-Like Films," H.W. White, Proc. of U.S. Army Applications for Diamond and Diamond-like Materials, Army Research Office, pp. 35-37, Conf. in Chapel Hill, NC, 13-14 June (1989).

"Surface Force Measurements on Picometer and Piconewton Scales," P.J. Bryant, H.S. Kim, R.H. Deeken and Y.C. Cheng, J. Vac. Sci. Technol. **A8**, 3502 (1990).

"Tunable Diode Laser Infrared Reflection Absorption Spectroscopy of Carbon Monoxide on Pt(111)," L.F. Sutcu, J.L. Wragg and H.W. White, Phys. Rev. B. **41**, 8164-69 (1990).

"The Influence of Moisture on Electrical Conductivity in Polyaniline," D. Bradford, D. Cowan, T. Marrero, H.W. White, J. Wragg, Bull. Amer. Phys. Soc., **35**, 197 (1990).

"Report of Research Needs for Coating Characterization," H. W. White, Workshop on Surface Science and Technology, Ed., J. Belilo and R. Reeber, Ann Arbor, MI, pp. 1-5, 7-9 November (1990).

"Characterization of Protective Films on Steel and Metal Matrix Composites," H. W. White, J.L. Wragg, R. Moore, and L. Chann, Workshop on Surface Science and Technology, Ed., J. Belilo and R. Reeber, Ann Arbor, MI, pp. 42-43, 7-9 November (1990).

"Scanning Tunneling Microscopy of Solid C_{60}/C_{70}," J.L. Wragg, J.E. Chamberlain, H.W. White, W. Krätschmer, and D.R. Huffman, Nature **348**, 623-4 (1990).

"Large-Scale, Periodic Features Associated with Surface Boundaries in STM Images of Graphite, J.E. Buckley, J.L. Wragg, H.W. White, A. Bruckdorfer, and D.L. Worcester, Jour. Vac. Sci. and Tech. B 9 (2), 1079-82 (1991).

"High Resolution Vibrational Linewidth Study of CO on Pt(111)," L.F. Sutcu, J.L. Wragg, and H.W. White, Surf. Sci. Lett. **249**, L343-46 (1991).

"In Situ Infrared Spectroscopy," J.L. Wragg and H.W. White, chap. in Surface and Interface Characterization in Corrosion, Ed., S. Shah, NACE, Houston, TX (in press).

"Tunable Diode IRRAS Study of CO on Pt(111)," H.W. White, L.F. Sutcu and J.L. Wragg, Proc. Conf. on Applied Spectroscopy in Materials Science II, Ed., William G. Golden, SPIE Vol. 1636, pp. 27-31, Los Angeles, CA, 20-22 January (1992).

"Force Microscopy Utilizing Tunnel Junction Control," H.S. Kim and P.J. Bryant , J. Vac. Sci. Tech. **A10**, 641 (1992).

"Current and Future Directions in Corrosion Research," H. W. White and J.L. Wragg, Proc. Tri-Service Conference on Corrosion, Plymouth, MA, 12-14 May (1992), Gordon A. Bruggeman, Conf. Chair, Milton Levy, Prog. Chair, U.S. Army Mat. Tech. Lab., Watertown, MA (In press).

"Past, Present and Future Developments in Optical Spectroscopies as Applied to the Characterization of Corrosion," H.W. White and J.L. Wragg, Paper to accompany Presentation #93352 at Corrosion/93, New Orleans, LA, 7-12 March 1993, NACE, Houston, TX (In press: To be published and available for purchase in single copy format by NACE).

"Mechanisms of Corrosion Protection by Cerium Based Surface Layers on Al 6061," J. L. Wragg, J. E. Chamberlain, R. L. Moore, H. W. White, F. Mansfeld and H. Shih, J. Electrochem. Soc. (submitted for publication).

"Raman Spectroscopy and Atomic Force Microscopy Studies of Zinc Phosphate and Polyacrylic Acid Complexed Zinc Phosphate Conversion Coatings on Steel," J. L. Wragg, L. Chann, J. E. Chamberlain, H. W. White, T. Sugama, and S. Manalis, J. Applied Polym. Sci. (submitted for publication).

"Atomic Force Microscope Designs," P.J. Bryant and H.S. Kim, J. Vac. Sci. Tech. A (submitted).

"Scanning Probe Microscopy Techniques Applied to Conducting and Non-Conducting Materials: C, MoS_2, Fe_2O_3, and an Organic Photoconductor," H.S. Kim and P.J. Bryant (manuscript in preparation).

"Atomic Structure and Electronic Structure Studies of CdTe by STM/STS," H.S. Kim and P.J. Bryant (manuscript in preparation).

"Raman and Atomic Force Microscopy Studies of Aluminum/Silicon Carbide Metal Matrix Composites," J. L. Wragg, J. E. Chamberlain, R. L. Moore, H. W. White, F. Mansfeld and H. Shih, J. Electrochem. Soc. (manuscript in preparation).

"Raman, Atomic Force Microscopy and *In Situ* Infrared Studies of High Performance Electrochemical Capacitor Electrodes," J. L. Wragg, J. E. Chamberlain and H. W. White, J. Electrochem. Soc. (manuscript in preparation).

IV. PRESENTATIONS

"Tunable Diode Laser Infrared Reflection Absorption Spectroscopy of Carbon Monoxide on Pt(111)," L.F. Sutcu, J.L. Wragg and H.W. White, 37th Midwest Solid State Conf., Univ. of Missouri, Rolla, MO, 13-14 October (1989).

"Techniques for Atomic Force Mapping," by H. Deeken and P.J. Bryant, 37th Midwest Solid State Conf., Univ. of Missouri, Rolla, MO, 13-14 October 1989.

"A Rugged Scanning Tunneling Microscope for Ultra High Vacuum," M.A. Pederson and P.J. Bryant, 37th Midwest Solid State Conf., Univ. of Missouri, Rolla, MO, 13-14 October 1989.

"Atomic Resolution Imaging of Novel Metal Thin Films by Scanning Tunneling Microscopy," H.S. Kim, Y.C. Zheng and P.J. Bryant, 37th Midwest Solid State Conf., Univ. of Missouri, Rolla, MO, 13-14 October 1989.

"Scanning Tunneling Microscopy and Raman Spectroscopy as Applied to Thin Film Analysis," J. Wragg, Chemical Engineering Department, Univ. of Missouri-Columbia, October (1989).

"Tunable Diode Laser Infrared Reflection Absorption Spectroscopy of Carbon Monoxide Adsorbed on Pt(111)," L.F. Sutcu, J.L. Wragg and H.W. White, Amer. Phys. Soc. Mtg., Anaheim, CA, 12-16 March (1990).

"The Influence of Moisture on Electrical Conductivity in Polyaniline," D. Bradford, D. Cowan, T. Marrero, H.W. White, J. Wragg, Presentation at Mtg. Amer. Phys. Soc. Mtg., Anaheim, CA, 12-16 March (1990).

"Raman Spectroscopy of Protective Films", J.L. Wragg and H.W. White, Presentation at Corrosion/90, Nat'l Assoc. of Corr. Eng. (NACE), Las Vegas, NV, 26 April (1990).

"Surface Analysis I&II," H.W. White, Plasma Polymerization & Plasma Surface Modification of Materials, Columbia, MO, 15-18 May (1990).

"Scanning Tunneling Microscopy of n-Alkanes Adsorbed on Graphite," J.E. Buckley, J.L. Wragg and H.W. White, Fifth Intern'l Conf. on Scanning Tunneling Microscopy/Spectroscopy and First Intern'l Conf. on Nanometer Scale Science and Technology, Baltimore, MD, 23-27 July (1990).

"Large-Scale, Hexagonally Arranged Features Associated with Surface Boundaries in STM Images of Graphite" J.E. Buckley, J.L. Wragg and H.W. White, Fifth Intern'l Conf. on Scanning Tunneling Microscopy/Spectroscopy and First Intern'l Conf. on Nanometer Scale Science and Technology, Baltimore, MD, 23-27 July (1990).

J. Wragg presented talks on "Micro-Raman Spectroscopy and STM for Surface Characterization" at the following universities during the period July - December (1990):

Pittsburg State University, Pittsburg, KS;
Southwest Missouri State Univ., Springfield, MO,
Southeast Missouri State Univ., Cape Girardeau, MO,
Southern Illinois Univ., Carbondale, IL,
Northeast Missouri State Univ., Kirksville, MO, and
Western Illinois Univ., Macomb, IL.

"STM, AFM and Vibrational Spectroscopy for Surface Characterization," J. Wragg, Department of Physics, Univ. of Missouri-St. Louis, 4 October (1990).

"Atomic Force Microscopy and Micro-Raman Spectroscopy of Composite Materials," J. Wragg, Chemical Engineering Department, Univ. of Missouri-Columbia, 8 October (1990).

"Corrosion Protection of Al Alloys and Al-based Metal Matrix Composites," by Florian Mansfeld, University of Michigan--ARO sponsored Workshop on Surface Science and Technology, Ann Arbor, MI, 7-9 Nov. (1990).

"Characterization of Protective Films on Steel and Metal Matrix Composites," H. W. White, J.L. Wragg, R. Moore, and L. Chann, in Workshop on Surface Science and Technology, Ann Arbor, MI, 7-9 November (1990).

"Report of Research Needs for Coating Characterization," H. W. White, in Workshop on Surface Science and Technology, Ann Arbor, MI, 7-9 November (1990).

"*In Situ* Infrared Spectroscopy", J.L. Wragg and H.W. White, Paper #77 in Corrosion/91, Nat'l Assoc. of Corr. Eng., Cincinnati, OH, 15 March (1991).

"Surface Analysis I&II," H.W. White, Plasma Polymerization & Plasma Surface Modification of Materials, Osage Beach, MO, 14-16 May (1991).

"Raman and Infrared Vibrational Studies of Adsorbates and Thin Films,", Sandia National Laboratories, Albuquerque, NM, 12 October (1991).

"High Resolution Vibrational Study of CO on Pt(111)," Department of Physics, University of Missouri-Kansas City, MO, 22 November (1991).

"Tunable Diode IRRAS Study of CO on Pt(111)," H.W. White, L.F. Sutcu and J.L. Wragg, in Conf. on Applied Spectroscopy in Materials Science II, at SPIE Int'l. Symp. on Lasers, Sensors, and Spectroscopy, Los Angeles, CA, 20-22 January (1992).

"Atomic Force Microscope Designs," P.J. Bryant and H.S. Kim, to be presented at the 39th National Symposium of the American Vacuum Society, Chicago, IL, Nov. 1992.

"Current and Future Directions in Corrosion Research," H. W. White and J.L. Wragg, Tri-Service Conference on Corrosion, Gordon A. Bruggeman, Conf. Chair, Milton Levy, Prog. Chair, Plymouth, MA, 12-14 May (1992).

"Past, Present and Future Developments in Optical Spectroscopies as Applied to the Characterization of Corrosion," H.W. White and J.L. Wragg, Presentation #93352 at Corrosion/93, New Orleans, LA, 7-12 March (1993).

V. Participating Scientific Personnel and Degrees Earned on Project

MU: Participating Personnel:

H. White, PI
J.Wragg, Graduate Student, PhD Candidate, Post Doctoral Fellow
Leyla Sutcu, Graduate Student, PhD Candidate
J. Chamberlain, Graduate Student, PhD Candidate
Lorin Chann Graduate Student, MS Candidate
R. Moore, Graduate Student, MS Candidate
K. Hamacher, Graduate Student, MS Candidate
J. Buckley, Undergraduate Student, BS Candidate
Sanjukta Misra, Undergraduate Student, BS Candidate
R. Roseman, Undergraduate Student, BS Candidate
M. Bullock, Summer Research Intern
C. Varon, Summer Research Intern
D. Esbenshade, Summer Research Intern

MU: Degrees Awarded:

Sanjukta Misra, BS, May 1990
Leyla Sutcu, PhD, May 1990
Lorin Chann, MS, December 1990
R. Moore, MS, May 1991

USC: Participating Personnel:

F. Mansfeld, PI
H. Shih, Res. Assist. Prof.
Y. Wang, Graduate Student, PhD. candidate.
F.J. Perez, Visiting Scientiest

USC: Degrees awarded: None.

UMKC: Participating Personnel:

P. Bryant, Assoc. PI;
H.S. Kim, Graduate Student, PhD candidate;
R.H. Deeken, Graduate Student, MS candidate.
Y.C. Cheng, Graduate Student, MS candidate

UMKC: Degrees awarded:

Y.C. Cheng, MS, May 1990
R.H. Deeken, MS, December 1990.
H.S. Kim, PhD, May 1992

VI. REPORT OF INVENTIONS

NONE

VII. BIBLIOGRAPHY

1. D. R. Arnott, B. R. W. Hinton and N. E. Ryan, *Corrosion* **45**, 12 (1989).
2. B.R.W. Hinton, D. R. Arnott and N. E. Ryan, *Mater. Forum* **7**, 211 (1984).
3. R. Arnott, B. R. W. Hinton and N. E. Ryan, in *Corrosion/88*, NACE, Houston, TX (1988) Paper No. 197.
4. F. Mansfeld, S. Lin, K. Kim and H. Shih, *Corr. Sci.* **27**, 997 (1987)
5. F. Mansfeld, S. Lin, K. Kim and H. Shih, *Corrosion/88*, NACE, Houston, TX (1988) Papers 380 and 382.
6. F. Mansfeld, V. Wang and H. Shih, *J. Electrochem Soc* **138**, L74 (1991).
7. F. Mansfeld, S. Lin, S. Kim and H. Shih, *J. Electrochem Soc* **137**, 78 (1990).
8. W. Vedder and D. A. Vermilyea, *Transactions of the Faraday Soc.* **65**, 561 (1969); A. Domony and E. Lichtenberger-Bajza, *Metalloberflache* **15**, 134 (1961). Summarized in "Advances in Corrosion Science and Technology," Vol 1,p. 276, M. G. Fontana and R. W. Staehle, Eds., Plenum, New York (1970).
9. F. Mansfeld and Y. Wang, manuscript in preparation.
10. A.J. Davenport, H. S. Isaacs and M. W. Kendig, *J. Electrochem. Soc.* **136**, 1837 (1989).
11. E. L. Ghali and J.J.A. Potvin, Corr. Sci. **12**, 583 (9172).
12. T. Sugama, L.E. Kukacka, N. Carciello and J.B. Warren, J. Appl. Polym. Sci. **30**, 4357 (1985).
13. T. Sugama, L.E. Kukacka, N. Carciello and J.B. Warren, J. Appl. Polym. Sci. **30**, 3469 (1986).
14. Digital Instruments, Inc. 6780 Cortona Drive, Santa Barbara, CA 93117.